Imaging Before Endoscopic Surgery

1

Margit Dueholm

Contents

1.1 **Introduction** 2

1.2 **Everyday, Perioperative Imaging in Endoscopy** 2

1.3 **Standardization on Performance of TVS, GIS and SIS, Doppler – Terms and Definitions** 2

1.3.1 Standardization of TVS 2

1.3.2 Saline Infusion Sonography (SIS) and Gel Infusion Sonography (GIS) 3

1.3.3 Three-Dimensional Transvaginal Ultrasound (3D-TVS) 5

1.3.4 Three-Dimensional Power Doppler Angiography (3D-PDA) 7

1.3.5 Dynamic Contrast-Enhanced MRI (DCE MRI) and Diffusion-Weighted MRI (DW MRI) 7

1.3.6 Contrast Enhanced Ultrasound (CEUS) 11

1.4 **Diagnosis of Uterine Pathology** 11

1.4.1 Abnormal Uterine Bleeding 11

1.4.2 Endometrial Pathology 11

1.4.3 Adnexal Masses 14

1.4.4 Power Doppler at TVS for Evaluation of Uterus and Adnexal Mass 16

1.4.5 Dynamic Contrast-Enhanced MRI (DCE MRI) and Diffusion-Weighted MRI (DW MRI) 16

1.5 **Evaluation of Congenital Uterine Abnormalities** 17

1.6 **Fertility Investigation** 17

1.6.1 Tuba Factor 18

1.7 **Observer Variation** 19

References 19

Abbreviations

2D	Two-dimensional
3D	Three-dimensional
3D-PDA	Three-dimensional power Doppler angiography
3D-TVS	Three-dimensional transvaginal ultrasound
ADC	Apparent diffusion coefficient
CEUS	Contrast-enhanced ultrasound
CT-scanning	Computer tomographic imaging
DCE MRI	Dynamic contrast-enhanced magnetic resonance imaging
DW-MRI	Diffusion-weighted magnetic resonance imaging
FI	Flow index
GIS	Gel infusion sonography
HSG	Hysterosalpingography
HY	Hysteroscopy
HyCoSy	Hysterosalpingo-contrast sonography
IETA	International Endometrial Tumor Analysis group
IOTA group	The International Ovarian Tumor Analysis group
JZ	Junctional zone

M. Dueholm
Department of Obstetric and Gynecology,
Aarhus University Hospital, Brendstupgaardsvej 100,
Aarhus N 8200, Denmark
e-mail: dueholm@dadlnet.dk

O. Istre (ed.), *Minimally Invasive Gynecological Surgery*,
DOI 10.1007/978-3-662-44059-9_1, © Springer-Verlag Berlin Heidelberg 2015

JZ_{diff}	Difference between maximal and minimal junctional zone thickness
JZ_{max}	Maximal junctional zone thickness
K^{trans}	Volume transfer constant
MRgFUS	Magnetic resonance-guided focused ultrasound
MRI	Magnetic resonance imaging
PET-CT	Positron emission tomography – computed tomography
RFA	Radiofrequency ablation of uterine myomas
RMI	Risk of malignancy index
SIS	Saline infusion hydrosonography
TVS	Transvaginal ultrasound
UAE	Uterine artery embolization
VFI	Vascularization-flow index
VI	Vascularization index

1.1 Introduction

During the last centuries diagnostic imaging has been followed by therapeutic imaging. Nowadays, therapeutic imaging is most often endoscopic surgery. Several newer procedures such as uterine artery embolization (UAE), magnetic resonance-guided focused ultrasound (MRgFUS), and radiofrequency ablation of uterine myomas (RFA) are examples of therapeutic imaging, which are not based on endoscopy.

Preoperative imaging should be seen as an integrated part of endoscopy that is absolutely needed to help the surgeon plan the type of surgery, and makes endoscopy safe and cost-effective.

Transvaginal ultrasound (TVS) is an easy accessible technique, and it is the first technique of choice in gynecologic diagnosis before endoscopic surgery. Simple gray-scale TVS is a sufficient imaging technique for most simple endoscopic procedures. A supplement to TVS of power Doppler, saline infusion hydrosonography (SIS) or gel infusion sonography (GIS) and three-dimensional transvaginal ultrasound (3D-TVS) may add valuable information.

TVS has limitations, where magnetic resonance imaging (MRI) should be added with different supplements. MRI is clearly superior to CT scanning for pelvic pathology, and CT scanning is not included in this section.

TVS is a very observer-dependent technique, and introduction of terms and standards increases the diagnostic performance of imaging (Kaijser et al. 2012). Terms and definitions for describing uterine and ovarian pathology have been developed (Leone et al. 2010; Munro et al. 2011; Timmerman et al. 2010). These terms should be adopted in the strategy of preoperative diagnosis and for operative planning.

In this chapter, we will give a schematic overview of these terms and details of the present performance of TVS and MRI before endoscopy and newer imaging procedures.

1.2 Everyday, Perioperative Imaging in Endoscopy

There are large advantages of incorporating image mapping immediately before and during endoscopic surgery. It is important to have an easy access to ultrasound equipment with sufficient resolution in the surgical units. Image documentation on still images may not give the surgeon the same information as is provided with a scan immediately before the surgery. Type 3 myomas may not be seen by either hysteroscopy (HY) or laparoscopy, and may be removed at ultrasonographic guidance at either HY (Lykke et al. 2012) or laparoscopy. Hysteroscopic resection of adenomyosis, asherman, septate uteri, and other uterine anomalies is performed more safely with ultrasound guidance, and perioperative TVS may guide the surgeon in the right direction in a frozen pelvis.

1.3 Standardization on Performance of TVS, GIS and SIS, Doppler – Terms and Definitions

1.3.1 Standardization of TVS

TVS is an operator-dependent technique, and should follow the sequences below:

(a) Optimization of the image. Four important buttons should be used at each examination (magnification, gain, focus, frequency)

(b) A systematic examination technique, as outlined below
(c) Pattern recognition of different pathologic conditions in the female pelvic, which should be described according to standardized terms and documented.

When additional information is needed:

(d) Addition of power Doppler (description according to standard terms and documentation)
(e) Addition of contrast (SIS or GIS) (description according to standard terms and documentation)
(f) Addition of 3D-TVS
(g) Addition of trained ultra-sonographer
(h) Addition of MRI
(i) Image conferences

The uterus is scanned in the sagittal plane from cornu to cornu and in the transverse plane from the cervix to the fundus. During examination assure the buttons are corrected to optimize visualization (magnification, gain, focus, frequency). Having established an overview of the whole uterus, the image is magnified to contain only the uterine corpus. The sagittal plane of the uterus is identified, and systematic scanning of the endometrium is performed using the terminology for the endometrium (Leone et al. 2010) in Table 1.1. The myometrium should be evaluated and described according to Table 1.2. The terms for myometrial lesions are built on terminology in prior studies (Dueholm et al. 2001c; Yaman et al. 1999; Champaneria et al. 2010; Meredith et al. 2009; Bazot et al. 2001), and the classification system for myomas is built on the FIGO system (Munro et al. 2011). The FIGO classification system for myomas is displayed in Fig. 1.1. In abnormal findings in the uterus, power Doppler may be added and described (Tables 1.1 and 1.2).

After evaluation of the uterus, the remaining pelvic area should be evaluated. The ovaries and the uterine horns should be located in the transverse plan. The tubes can be followed from the uterine horns to the iliac vessels and these procedures will normally reveille the ovaries. Each ovary should be scanned in the transverse and sagittal plane from the bottom to top and scanning should be performed in two perpendicular planes. Areas above, beneath and besides the ovaries should be scanned at each side.

The ovaries should be described according to standard terms from the International Ovarian Tumor Analysis (IOTA) group (Timmerman et al. 2000, 2010) (Table 1.3). Again power Doppler may be added in the evaluation of abnormal findings. The urinary bladder and the pouch of Douglas should be evaluated. Sliding of different organs (gentle movement with the probe) should be noted. The urinary bladder, the rectum, and sacrouterine ligaments are also scanned and recorded.

In endometriosis, visualization of the relationship with the vaginal wall and the rectum may be important to diagnose rectal involvement (Hudelist et al. 2011). To evaluate deep rectovaginal endometriosis, the probe should be placed on the posterior cul de sac of the vagina, and when the probe is slowly withdrawn through the vagina the utero sacral ligament, posterior fornix and the rectovaginal septum can be visualized. By gentle movement of the probe the rectal mucosal and the recto sigmoid wall can be identified and evaluated for deep infiltrating endometriosis. Visualization may be increased by large amounts of gel in the vagina.

1.3.2 Saline Infusion Sonography (SIS) and Gel Infusion Sonography (GIS)

Negative contrast agent such as saline or gel can increase the visualization and outline of abnormalities in the uterine cavity at TVS. Polyps, myomas, synekia, cesarean section scars, and uterine anomalies are often more clearly visualized by contrast in the uterine cavity. When saline is used as contrast agent, it is called saline infusion sonography (SIS), while the use of gel as contrast agent is called gel infusion sonography (GIS).

1.3.2.1 Submucous Myomas for Hysteroscopic Surgery

Submucous myomas for hysteroscopic surgery may at GIS/SIS be evaluated as outlined in Table 1.2 and displayed in Fig. 1.2, and may be scored by the STEPW system to predict complexity of surgery (Lasmar et al. 2011) (Table 1.2). The STEPW system consists of the following

Table 1.1 Systematic scanning of the uterine endometrium, with application of common terms and measurements for description of abnormalities

TVS		Terms and measurements
In the sagittal the endometrial thickness is measured		"Double endometrial thickness"
Intracavitary fluid: the thickness of both single layers are measured and the sum is recorded as the maximum measurement in the sagittal plane		Endometrial thickness
Amount of intracavitary fluid: largest measurement in the sagittal plane		Largest measurement of fluid
Echogenicity of fluid		Anechogenic, low-level echogenicity ground glass
		Mixed echogenicity
Endometrial morphology		
Endometrial echogenicity compared to the myometrium		Hyper-, iso- or hypoechogenic
Homogeneous with symmetrical anterior and posterior sides (includes the three-layer pattern, and the homogeneous hyper-, hypo- and isoechogenic endometrium)		Uniform
Heterogeneous, asymmetrical or cystic endometrium		Not uniform
The endometrial midline is described	Straight hyperechogenic interface	Linear
	A waved hyperechogenic interface	Non-linear
	Irregular interface	Irregular
	Absence of a visible interface.	Not defined
The endometrial–myometrial junction		Regular, irregular, interrupted or not defined
An echo formed by the interface between an intracavitary lesion and the endometrium		Bright edge
Intracavitary pathology		
Endometrial thickness including the lesion is measured (not including intracavitary myoma)		
Intracavitary lesions should be measured in three perpendicular diameters (d1, d2, d3)		d1, d2, d3
The volume (V) of the lesion may be calculated from the three orthogonal diameters ($d1 \times d2 \times d3 \times 0.523$)		V
Myoma measurement (Table 1.2)		
Synechiae are defined as strands of tissue crossing the endometrium		Synechia
Color Doppler assessment of the endometrium		
The color content of endometrium can be scored: (1) no color flow; (2) with minimal color; (3) moderate color; (4) abundant color is presented		Color score 1 to 4
Vascular pattern:		
Scattered (dispersed color signals within the endometrium but without visible origin at the myometrial–endometrial junction) or not scattered vessels		Scattered, not scattered
Dominant vessel: one vessel passing the endomyometrial junction		Dominant, not dominant
Caliber of vessels		Large or small
Vessels may be single (double) or multiple, with focal or multifocal origin or there might be circular flow		Single (double), multiple focal, multifocal, circular flow
Branching of vessels		Orderly or disorderly/chaotic
GIS or SIS		
The endometrial outline		
Appears regular		Smooth
Multiple thickened "undulating" areas, "moguls" with a regular profile		Endometrial folds
Deep indentations or		Polypoid
Surface is cauliflower like or sharply toothed ("spiky")		Irregular

Table 1.1 (continued)

Intracavitary lesions:	
Extended: Lesion involves ≥ 25 % of the endometrial surface	Extended
Localized: Lesion involves < 25 % of the endometrial surface	Localized
Pedunculated: *a*/*b* ratio is <1; Sessile: : *a*/*b* ratio is ≥ 1	Pedunculated, sessile
a/*b* ratio between the diameter of the base level of the endometrium (*a*)	
Maximal transverse diameter of the lesion (*b*)	
The echogenicity of a lesion is defined as "uniform" (homogenic) or	Uniform
"Nonuniform" (heterogenic), which includes cystic lesions	Not uniform
The outline of the lesion is defined as "regular"	Regular
or "irregular" (e.g. spiky or cauliflower like)	Irregular

five parameters, where a score of 0–2 is given according to Table 1.2:

(a) *Size*: Myomas (largest diameter)
(b) *Topography*: Defined by the third of the uterine cavity where the myoma is situated (lower, middle and upper third).
(c) *Extension of the base of the myoma*: Base of myoma covers (one-third of the wall, one- to two-thirds of the wall, and more than two-thirds of the wall).
(d) *Penetration of the myoma into the myometrium*: Type 0,1,2 myoma
(e) *Wall*: when the fibroid is on the lateral wall, one extra point is added.

The total sum score predicts complexity of hysteroscopic surgery.

1.3.3 Three-Dimensional Transvaginal Ultrasound (3D-TVS)

3D-TVS is just a collection of 2D images added together in a volume, which allow reconstruction and evaluation of the scan in different planes. Resolution at 3D will never be better, than at the original 2D images. In the presence of poor image quality at 2D, a collection of images of poor quality at 3D will seldom be helpful. Most important feature at 3D–TVS is the ability to "reconstruct" the uterus to provide a coronal view.

Procedure: For 3D-TVS of the uterus, volumes are obtained at a mid-sagittal view of the uterus. The image settings at 2D should be optimized, and magnified to an optimal image with a minimum amount of free space around the region of interest (uterus). The volume box for sampling of the 3D images should be applied again with a limited amount of free space around the uterus. Both the patient and the probe should not be moved during collection of the volumes.

To obtain a reconstruction of the coronal plane, the volume of the uterus should be perfectly aligned along the mid long axis in the sagittal plane and along the axis of the uterine horns in the transverse planes. This can be achieved by the Z-technique (Abuhamad et al. 2006), which include three steps (Fig. 1.3).

The time spent on producing a perfect coronal view is less than 1 min after limited training (Abuhamad et al. 2006). A perfect coronal view and a simple scroll through the images in the C-plan may in clinical practice supply most additional information given by 3D-TVS.

There is a substantial learning curve and time involved to manage all the different features in post-processing, which limits the common use in clinical practice. However, two or three features can easily be learned and may in most clinical situations cover the need.

At SIS a 3D volume of the uterus can be obtained (3D-SIS), which allow reconstructing the outline of the uterine cavity. However, an optimal reconstruction without acoustic shadows from an intrauterine catheter is achieved with gel in the uterine cavity, and the catheter should be removed before volume sampling (3D-GIS). 3D-GIS may be helpful in some clinical situations especially in indefinite coronal view at 3D-TVS (Mavrelos et al. 2011; Caliskan et al. 2010; Makris et al. 2007; de Kroon et al. 2004).

Table 1.2 Qualitative assessment of myometrium and myometrial lesions (myomas and adenomyosis)

	Definition	Term, measurement
Uterine contour	Normal: pear shape; globular: globally enlarged; bernoccolute: uterus with irregular external profile	Normal, globular, bernocculuto
Uterine volume	Length (d1), anterior posterior diameter (d2) and transverse diameter (d3)	$(d1 \times d2 \times d3 \times 0.523)$
Uterine perimetrial outline	Regular: smooth with a regular shape; irregular: not smooth contour	Regular, irregular, not defined
Myometrial wall	Measurement of anterior and posterior wall thickness in sagittal plane	Symmetrical, asymmetrical maximal thickness of wall
Myometrial echogenicity	Homogenous	Uniform
	Heterogenous, or cystic	Non-uniform
	Regular cystic or not regular cystic	Cystic
Junctional zone	Hypoechogenic inner subendometrial halo	Regular, irregular, interrupted, not defined
Myometrial lesions		**Presence, number, shape**
Contour	Clear hypo or hyperechoic external contour (rim)	Rim defined, not defined
Margins	Defined margins	Regular, irregular
Echogenicity	Hypo, iso, hyperechogenic (+/− shadows)	Uniform
	Heterogenic mixed echo, cystic areas, lacunae, stripes, shadows	Not uniform
Site		Anterior, posterior wall
Location		Middle site or lateral (right, left, corneal or intra ligamentar)
		Fundus, corpus, isthmus, cervix
	The minimal distance between the perimetrium and the outer portion of myoma (dm). The minimal distance between the endometrium and the inner portion of the myometrium (de)	dm de
	Submucous myomas extension of the base: proportion of wall covered	≤1/3; 1/3–2/3;>2/3
Type	Submucous (sm)	Type: 0,1,2
	(Type 0), myoma completely within the cavity; (Type 1) with ≥50 % of the endocavitary portion protruding into the cavity; and (Type 2), with the endocavitary part of myoma <50 %	
	Other (O)	Type: 3,4,5,6,7,8
	Contacts endometrium; 100 % intramural	Type 3
	Intramural	Type 4
	Subserosal ≥50 % intramural	Type 5
	Subserosal <50 % intramural	Type 6
	Subserosal pedunculated	Type 7
	Other (Specify, e.g. cervical, parasitic)	Type 8
	Hybrid impact on both endometrium and serosa	Type: 0–5
Size	The three largest perpendicular diameters (a1, a2, a3) mm	a1, a2, a3
	$1/6 \times \pi \times a1 \times a2 \times a3$	Volume
	$P = 6\ A^2\ (B/2 - A/3)/B^3$ B largest diameter perpendicular to the uterine cavity and A part of this diameter in the uterine cavity	P = Proportion of myoma volume in uterine cavity
Doppler morphology	Regular vessels or irregular vessels	Regular or irregular
	Branching: regular, irregular, no branching	Regular branching

Table 1.2 (continued)

		Definition					Term, measurement
		Scattered dispersed color signal					Scattered
		Many vessels					Multiple pattern
		Caliper, number					Large, small, few, many
		Homogenic vessels, size					Homogenic
		Peripheral					Circular or not circular flow
		Color score: (1) no color flow; (2) with minimal color; (3) moderate color; (4) abundant color is presented					Color score 1–4
STEPW		Submucous classification for complexity of hysteroscopic surgery					
	Score	Size	Topography	Extension of base	Myoma type	Lateral wall	
	0	<2	Low	<1/3	0 (100 %)	+1	
	1	2–5	Middle	1/3–2/3	1 (>50 %)		
	2	>5	Upper	>1/3	2 (<50 %)		
	∑	+	+	+	+	+	∑ Total score (SUM)
SUM	0–4	Low complexity hysteroscopy					
	5–6	High complexity hysteroscopy, two steps, medical preoperative treatment					
	7–9	Consider alternatives					

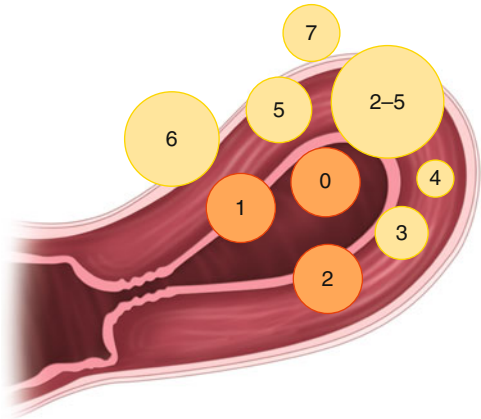

Fig. 1.1 In the FIGO system intracavitary myomas are classified by the traditional European Society for Gynaecological Endoscopy (ESGE) (type 0–2), and in addition intramural myomas are classified (type 3 to 7). Myomas with impact on both the endometrium and serosa are classified as type 2–5

1.3.4 Three-Dimensional Power Doppler Angiography (3D-PDA)

A three-dimensional power Doppler angiography (3D-PDA) can be performed to study the distribution, pattern, and vascular branching of the vascular vessels. Power Doppler is simply applied to the volume box and a 3D volume is obtained. The technique also allow for a more objective reproducible (Raine-Fenning et al. 2003) assessment of uterine vascularization, although the measurement is dependent on machine settings (Raine-Fenning et al. 2008).

1.3.5 Dynamic Contrast-Enhanced MRI (DCE MRI) and Diffusion-Weighted MRI (DW MRI)

Tissue perfusion in pelvic masses and uterine masses can be evaluated by DCE MRI (Nakai et al. 2008; Paldino and Barboriak 2009). In tissue with high perfusion there will be high signal intensity in T2-weighted images after injection of contrast, while tissue without perfusion will have low intensity at T2-weighted images. Tissue perfusion can be assessed in two ways: a semi-quantitative method (dependent on individual system and patients) which analyze the changes in signal intensity, and a quantitative method using a pharmacokinetic system and patient-independent model.

Diffusion-weighted (DW) MRI is based on diffusion motion of water molecules. Signals are

Table 1.3 Terms in definition of ovaries and ovarian mass

	Definitions	Measurements and terms
Size, site	Ovarian measurement: three perpendicular planes largest 3 diameters (mm) (a1, a2, a3)	a1,a2,a3
Ovarian volume		(a1 × a2 × a3 × 0.523).
Outline of ovary		Regular, irregular
Morphology of ovarian tissue		
	Follikels (numbers (n) and size in largest perpendicular diameters (A1, A2, A3) (mm)	N, A1, A2, A3
Antral follicle count	Count follicles between cycle days 2 and 4 Include all antral follicles of 2–10 mm in diameter (most reliable in 3D volume) in both ovaries	Antral follicle count
	Ovarian stroma	Homogenic Heterogenic
Measurements of ovarian mass (inconsistent in normal ovarian function)	Measurement of the ovarian mass in three perpendicular planes (b1, b2, b3) largest diameter in mm	b1, b2, b3
Morphology of mass	Echogenicity of solid component Solid: high echogenicity suggesting presence of tissue	Heterogenic or homogenic Cystic or solid or Cystic-solid
Cystic content		Anechogenic Low level Ground glass Hemorrhagic Mixed
	Septum complete/incomplete Thin strands of tissue running across the cyst cavity An incomplete septum is not completed in some scanning planes	Complete Incomplete
	The thickness of thickest septum (S) is measured	Thickness septum (S)
Locules	Numbers of locules (L) is counted	L
Internal wall		Smooth, irregular
	Any solid projection from the cystic wall ≥3 mm	Solid papillary projections
	Measurement of largest solid component in three perpendicular planes (height(h), base(ba1), base(ba2))	Height(h), base(ba1), base(ba2)
Cyst type	(No septae and no solid parts) No septae, but solid parts More than one septae, no solid parts More than one septae, and solid parts	Unilocular Unilocular solid Multilokular Multilokular solid Not classifiable
Doppler assessment	Color score: (1) no color flow; (2) with minimal color; (3) moderate color; (4) abundant color is presented	Color score 1–4
Ascitis	Presence of ascites is noted, largest pouch of fluid in pouch of Douglas is measured (F) in a saggital plane largest diameter (mm)	F

dependent on microscopic water diffusivity, and decrease in the presence of factors that restrict water diffusion, such as cell membranes and the viscosity of the fluid. Signals are influenced by changes in the balance between extracellular and intracellular water molecules, and changes in cytologic morphology including the nuclear-to-cytoplasm ratio and cellular density. The technique can easily be added to any routine MR protocol.

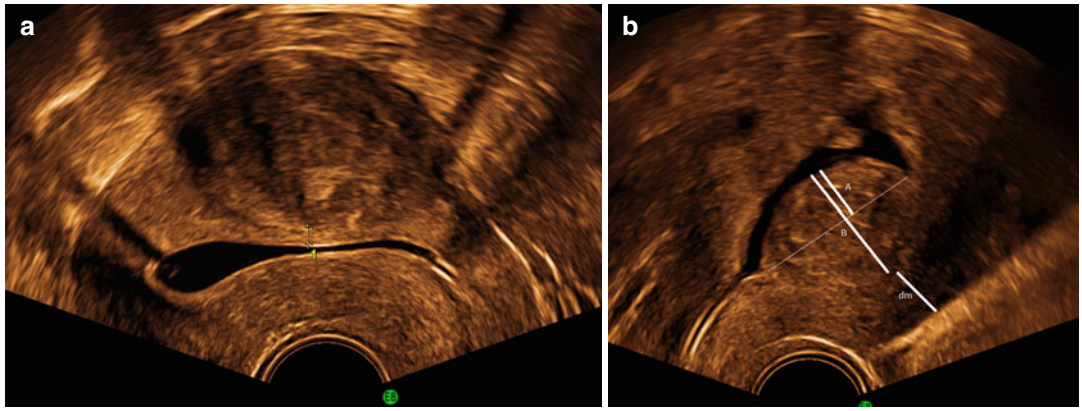

Fig. 1.2 A myoma type 2–5 (**a**) with impact on the serosa and endometrium (SIS), and (**b**) a myoma type 2 with measurement of the proportion of the myoma in the uterine cavity (P). *B* is largest diameter perpendicular to the uterine cavity and *A* is part of this diameter in the uterine cavity $P = 6\ A^2\ (B/2 - A/3)/B^3$

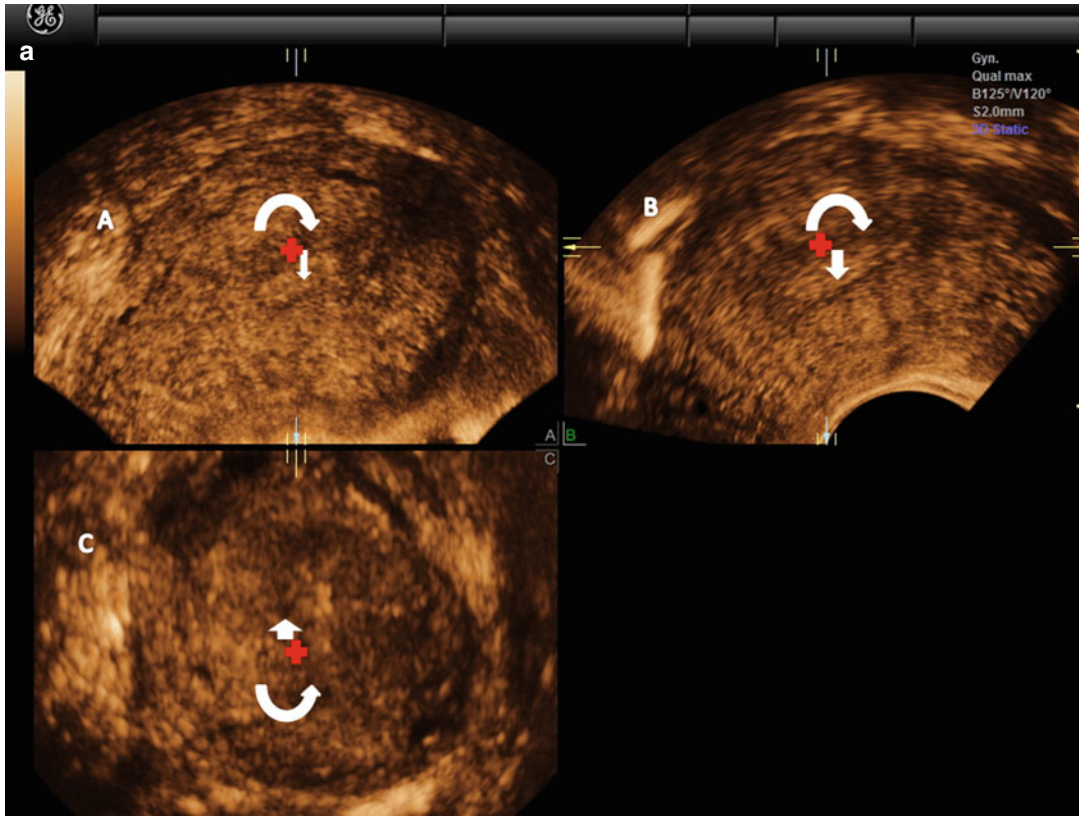

Fig. 1.3 (**a**) Step *A*. The reference/rotational point (+) is placed in the midlevel of the endometrial stripe in the sagittal plane. Z rotation is used to align the long axis of the endometrial stripe along the horizontal axis in the sagittal plane of the uterus. Step *B*. The reference/rotational point (+) is placed in the midlevel of the endometrial stripe in the transverse plane. The Z rotation is used to align the endometrial stripe with the horizontal axis in the transverse plane of the uterus Step *C*. Z rotation is applied on plane C to display the mid coronal plane in the traditional orientation in plane C. (**b**) In the C plane is the coronal view displayed (VCI-settings). (**c**) Postprocessor rendering is performed

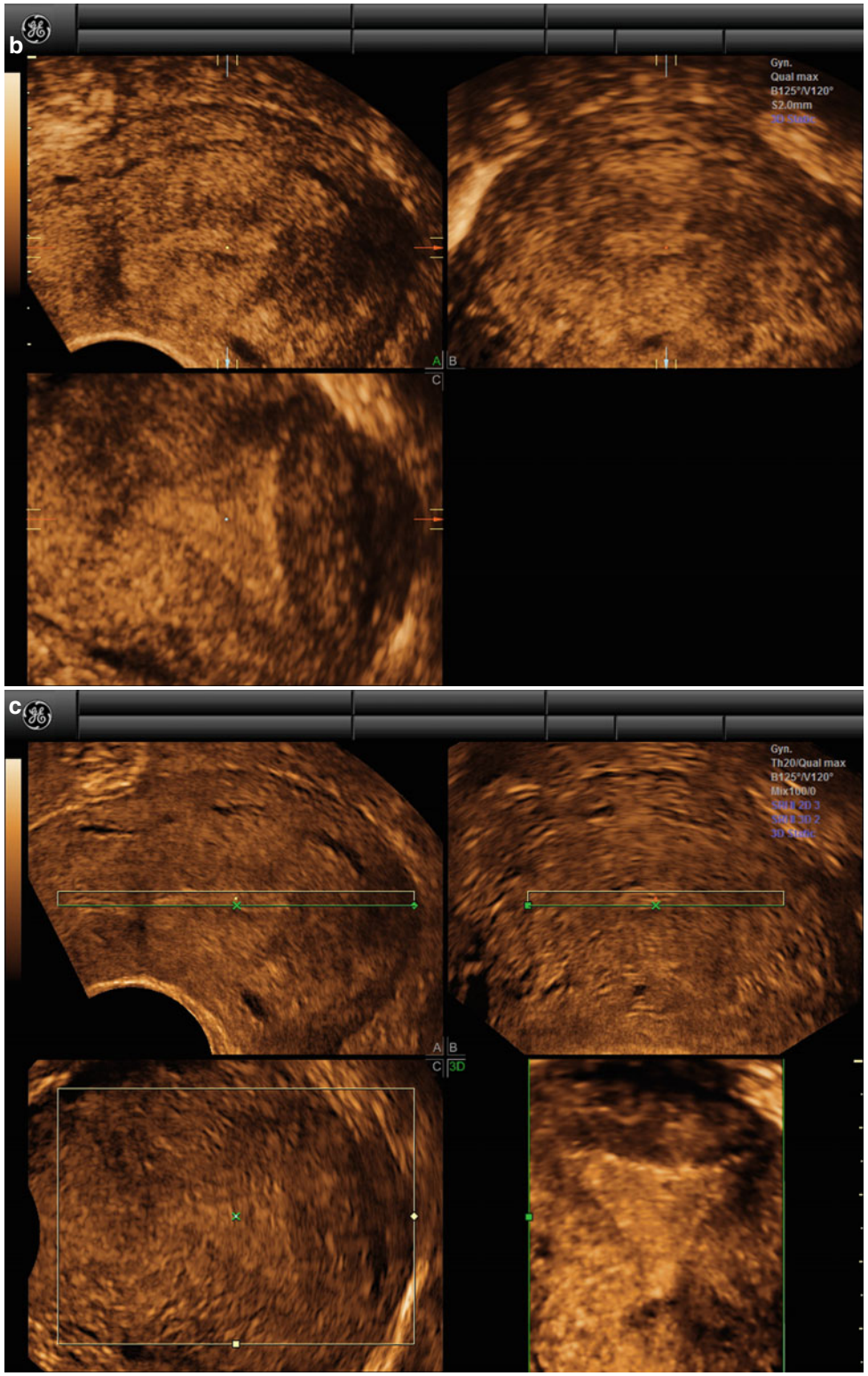

Fig. 1.3 (continued)

1.3.6 Contrast Enhanced Ultrasound (CEUS)

CEUS is an alternative upcoming method with use in other specialties (Piscaglia et al. 2012), to evaluate perfusion after different treatment modalities. CEUS has been used when HIFU has been monitored by TVS, and seems to be a promising low cost method (Zhou et al. 2007). Enhancement in the tissue is observed after contrast injection supported with in-built or off-line software to measure the degree of enhancement. The time of enhancement and the distribution is observed.

1.4 Diagnosis of Uterine Pathology

1.4.1 Abnormal Uterine Bleeding

The newly established FIGO system – the PALM-COIN ((P) polyp, (A) adenomyosis, (L) leiomyoma, (M) malignancy/hyperplasia-(C) Coagulopathy, (O) Ovulatory dysfunction, (I) Iatrogenic, and (N) Not classified) system – has been elaborated (Munro et al. 2011).

A patient with abnormal uterine bleeding should be categorized according to this system. The PALM – part of the system – is mainly based on ultrasound and pathologic evaluation of the endometrium. The COIN – part of the system – is evaluated by the patient history and laboratory analysis.

1.4.2 Endometrial Pathology

1.4.2.1 Premenopausal Bleeding

TVS, GIS, or SIS are very efficient methods to rule out pathology in the uterine cavity as polyps and myomas in premenopausal bleeding. To rule out polyps and myomas, TVS seems to miss one in five endometrial polyps (de Kroon et al. 2003; Dueholm et al. 2001a, b), while SIS is in line with hysteroscopy (HY). TVS is able to identify myomas, but a differentiation between myomas of type 1–3 most often require GIS/SIS, which is important for selection of myomas for either laparoscopic or hysteroscopic treatment (Dueholm et al. 2002a). Patients with symptomatic focal pathology will have a time-efficient planning of HY by TVS supplied with SIS or GIS. This will provide clear information of the size, number and type of pathology in the uterine cavity, and thereby patients can be selected for outpatient mini-hysteroscopy at an office setting, two-generation endometrial ablation, inpatients resectoscopic surgery, and also to surgeons with the required experience. Small intrauterine pathology with diameter below 2 cm (Bettocchi et al. 2004; Cicinelli 2010) is removed at outpatient mini-hysteroscopy. The complexity of resectoscopic hysteroscopic myoma surgery can be predicted by the findings at SIS/GIS and scored by the STEPW system (Table 1.2). Complex surgery (score five or more) should be performed by experienced surgeons, and a two-step procedure and preoperative medical treatment should be considered. UAE or laparoscopic myomectomy should be taken into account at scores of more than 7–9.

1.4.2.2 Postmenopausal Bleeding

TVS is the first investigation in postmenopausal bleeding. The endometrium should be investigated and described according to Table 1.1. Figure 1.4 shows examples of heterogenic (a) and cystic endometrium (b). In the presence of a sharp well-defined midline echo with endometrial thickness of ≤3 or ≤4 mm only 2 % respective 5 % of endometrial cancers will be missed (Timmermans et al. 2010). At an endometrial thickness >3–4 mm endometrial sampling is performed (Timmermans et al. 2010).

Neither systematic reviews nor international guidelines have been able to reach consensus regarding the sequence in which TVS, SIS/GIS endometrial samples and HY should be implemented in the diagnostic set-up (van Hanegem et al. 2011).

HY is more efficient than endometrial samples (van Hanegem et al. 2011) and there is lower efficiency of endometrial sampling in the presence of focal changes of the endometrium

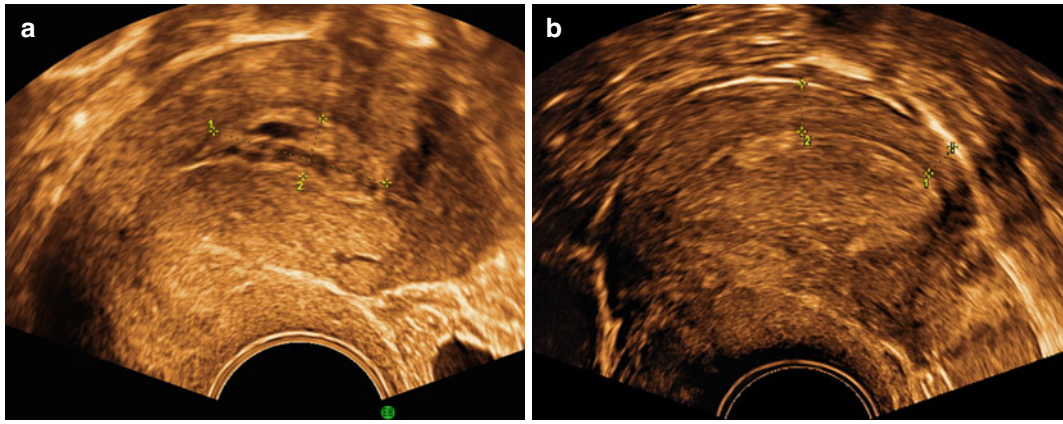

Fig. 1.4 A cystic polyp is seen in (**a**) with cystic regular endometrium, clear margins and bright line. A single small vessel was seen at Doppler. In (**b**) endometrial cancer, with a thickened heterogenic endometrium with regular endomyometrial junction at the posterior wall, (*marked*), but irregular not defined margins at the anterior wall

(Epstein et al. 2001; Angioni et al. 2008). This has motivated a supplement of SIS to TVS at endometrial thickness >5 mm, and to offer HY to patients with focal pathology at SIS (Epstein et al. 2002). The size of focal pathology can be clearly depicted at SIS/GIS and allows selection of office mini-hysteroscopy (Lotfallah et al. 2005; Cicinelli et al. 2003) for most minor pathology.

There has been limited attention on implementation of imaging for staging malignancy in a time-efficient diagnostic set up not only to diagnosis but also to fulfilled minimally invasive laparoscopic treatment of both benign and malignant pathology. Preoperative staging has the advantage of an efficient operative planning of a minimal invasive surgical procedure. An efficient preoperative diagnosis has been either additional TVS or MRI (Kinkel et al. 1999, 2009). HY may give important information of tumor type and cervical involvement (Cicinelli et al. 2008; Avila et al. 2008). The aspect of staging has to be implemented in the diagnostic set up during the next years.

1.4.2.3 Diagnosis of Myometrial Pathology

The diagnostic criteria for differentiation between the most common different myometrial abnormalities are outlined in Table 1.4, and examples are given in Fig. 1.5.

Unclassified ovarian and pelvic masses should primarily be seen by a trained sonographer. MRI may be indicated, and should be performed by a MRI specialist in pelvic MRI (Sect. 1.3.5).

TVS has the same diagnostic efficiency as MRI in experienced hands in differentiation between myomas and adenomyosis (Champaneria et al. 2010). However, MRI may be superior when experienced sonographers are not at hand, in indefinite cases at TVS, and when adenomyosis are present together with myomas (Bazot et al. 2001; Dueholm et al. 2001c).

1.4.2.4 Selection of Patients with Myomas for Endoscopy and Image-Guided Procedures

Selection of patients for different newer myoma treatment modalities is a developing specialty. The most common alternatives are UAE, RFA, and MRgFUS. The efficiency of UAE is well established, with good long-term outcome (Walker and Barton-Smith 2006).

MRgFUS is the only technique which is totally noninvasive. Focused ultrasound is applied to myomas guided by MRI, and myomas are ablated by thermal energy. This technique has efficient long- to midterm outcome (Stewart et al. 2007), and even pregnancy rates are encouraging (Rabinovici et al. 2010). The main disadvantage is the dependence on a costly new technology,

Table 1.4 TVS and MRI characteristics of most common myometrial masses

TVS	
Regular defined margin, edge shadows, echo dense, homogeneous, hypoechogenic, circular flow, regular or scattered vessels	Typical leiomyoma
Regular well-defined margins, edge shadows, heterogenic echogenicity with anechogenic, or mixed echogenicity and circular flow, regular or scattered vessels	Atypical leiomyoma
Irregular heterogenic echogenicity, irregular anechoic areas of necrosis, irregular margins, vessels irregular, regular or scattered	Neoplasme suspect myometrial lesion
Globular uterus, with asymmetric myometrial walls. Margins: Irregular poorly described. Echogenicity: heterogeneity, hypo- or hyperechogenicity. Distinct features: Linear striations, indistinct endomyometrial junction, hyperechogenic dots, anechogenic lacunae or cysts and irregular widening of the junctional zone. Vessels: Perpendicular vessels and limited circular flow	Probably adenomyosis
MRI	
Low signal intensity on T2-weighted images, and possible high intensity rim	Leiomyoma
Cystic degeneration: cystic, high intensity (T2) and myxoid degeneration: lobular, septate process, high intensity (T2), red degeneration: heterogenic mass of ten high intensity at the rim, late enhancement	Atypical leiomyoma
Large regular asymmetric uterus without myomas, ill-defined low signal intensity myometrial areas, heterotopic endometrial tissue (foci of increased high signal intensity in the junctional zone (JZ)). Ratio max >40 (JZmax/myometrial thickness), maximal junctional zone thickness. (JZmax) of 12 mm, (JZdif) difference of >5 mm between maximum and minimum JZ thickness (degree of irregularity)	Adenomyosis
Large broad based bulky polypoid mass, filling the uterine cavity, heterogeneous hypointense signal on T1-weighted images and hyperintense signal (T2), hemorrhage, (areas of elevated T1 signal), necrosis (foci of hyperintense signal (T2) myometrial invasion and heterogenic enhancement)	Carcinosarcoma/ adenosarcomas
Large heterogeneously enhancing mass, with central (T2) hyperintensity (necrosis). Hemorrhage (areas of elevated T1 signal), calcifications may be present. Early contrast enhancement, marginal irregularity (50 %). Alternatively, homogeneously low-signal mass, similar to a leiomyoma	Leiomyosarcomas

and that the technique only is applicable in limited numbers of myoma cases (Taran et al. 2010; Behera et al. 2010).

Needle-guided ablation can be performed with cryotherapy, focused ultrasound, and RFA. At RFA a needle is introduced into the fibroids guided by ultrasound, and radiofrequency energy is applied to the needle causing ablation of the fibroid. There is limited experience with this technique (Iversen et al. 2012; Kim et al. 2011; Garza Leal et al. 2011), but the midterm outcome is promising, and RFA seems to be a low cost simple alternative to MRgFUS.

In the individual patient the total numbers of myomas and their correct location have to be mapped before selection of patients for endoscopic treatment, UAE, RFA, or MRgFUS. It is without larger problems done by TVS when image quality is good. However, in the presence of several myomas (four or more), there might be more myomas in the acoustic shadows at TVS and MRI should be considered (Dueholm et al. 2002b). Patients with several to numerous small myomas could most efficiently be treated by UAE, while laparoscopic myomectomy is most often preferred for patients with larger subserous myomas (type 6–7), where none of the newer methods are optimal.

Submucous myomas with score below 5 in the STEMW system are treated with hysteroscopic resection, but there are often both submucous and intramural myomas. Submucous myomas are not optimally treated by MRgFUS or RFA (Iversen et al. 2012; Taran et al. 2010), but they are not any hindrance for UAE. However, there might be more infectious morbidity and prolonged discharge (Walker et al. 2004; Spies et al. 2002), and HY may be needed in the follow-up period after treatment.

TVS is a very efficient technique to roughly sort patients for modern image techniques, but

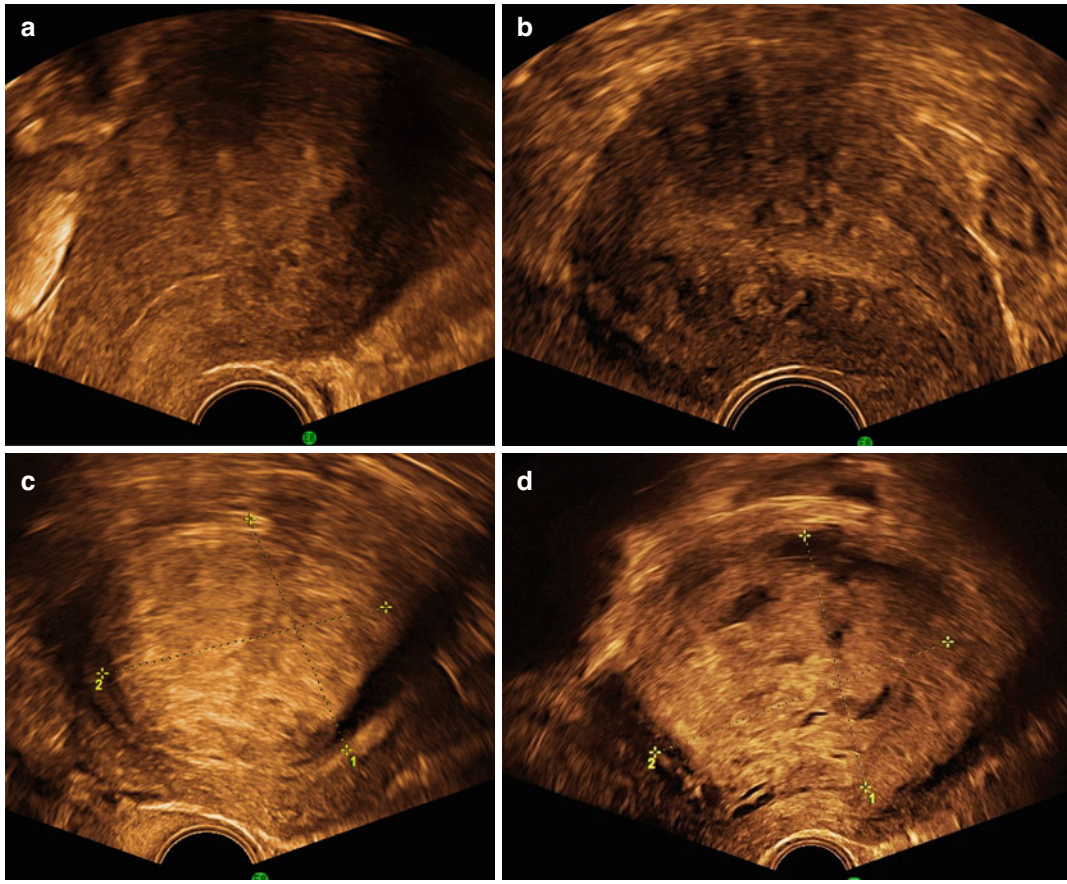

Fig. 1.5 Two typical examples of adenomyosis at TVS are displayed in (**a**) and (**b**). Both have irregular margins and not uniform echogenicity, and linear striation (**a**) with clear islands of ectopic endometrium and cysts, while the presence of adenomyosis in (b) is characterized with muscular hypertrofia, and small anechoic lacunae. (**c**) A typical well circumscribed myoma with regular margins, a hyperechoic rim, and uniform echogenicity. (**d**) An atypical myoma hyaline degenerated myoma with regular margins without a rim not uniform echogenicity, with irregular cystic spaces

MRI should be performed before definite treatment with UAE, MRgFUS, or RFA. It may have a higher efficiency for selection of patients than ultrasound (Spielmann et al. 2006), which probably is very observer-dependent. However, most important is valuable information on myoma vascularity given by MRI (see Sect. 1.3.5).

1.4.3 Adnexal Masses

TVS is the standard imaging for adnexal masses (ACOG 2007). These masses should in premenopausal women be described according to Table 1.3 which display the IOTA terms. Premenopausal adnexal masses should be handled according to the traditional risk of malignancy index (RMI) (RCOG.(11)) or IOTA rules (Table 1.5). (The two left column are the IOTA rules, and the left three display RMI in table 1.5.) In premenopausal women, newer studies (Kaijser et al. 2012; Timmerman et al. 2010) seem to show higher efficiency of the IOTA system (Van et al. 2012a, b). Corpus luteums, endometriomas, dermoids, fibroids, and hydrosalpinges are recognized by the specific pattern in the hands of trained sonographers (Sokalska et al. 2009). Figure 1.6 displays examples of adnexal masses.

RMI, which include Ca-125 may still provide the highest diagnostic efficiency in postmenopausal women (RCOG.(11)). Ca-125 has a low specificity in premenopausal women

Table 1.5 Classification of ovarian mass (IOTA rules left, RMI right)

IOTA rules		**RMI**		
B features *Benign*	*M features* *Suspect tumor*	Menopausal status (*M*)	Premenopausal Postmenopausal (hysterectomy >50 years)	0 3 *M* score
(1) Unilocular cyst;	(1) Irregular solid tumor;	Ultrasound score (*U*)	Unilokular > Bilokular	0 1
(2) Presence of solid components (largest solid component is <7 mm in largest diameter)	(2) Ascites; and		Solid areas Bilateral	1 1
(3) Acoustic shadows	(3) At least four papillary structures;		Excrescences Ascites	1 1
(4) Smooth multilocular tumor less than 100 mm in largest diameter; and	(4) Irregular multilocular – solid tumor (largest diameter >100 mm)		Extra-ovarian disease	1
(5) No detectable blood flow (color Doppler)	(5) Very high color content (color Doppler)	$\sum U$ score		$\sum U$ score
If one or more M features were present in the absence of a B feature, we classified the mass as malignant (rule 1)	If one or more B features were present in the absence of an M feature, we classified the mass as benign (rule 2)	Ca-125	Value	Ca-125
Not classifiable				
If both M features and B features were present, or if none of the features was present, the simple rules were inconclusive (rule 3)		RMI	RMI = M-Score × U-Score × CA-125	

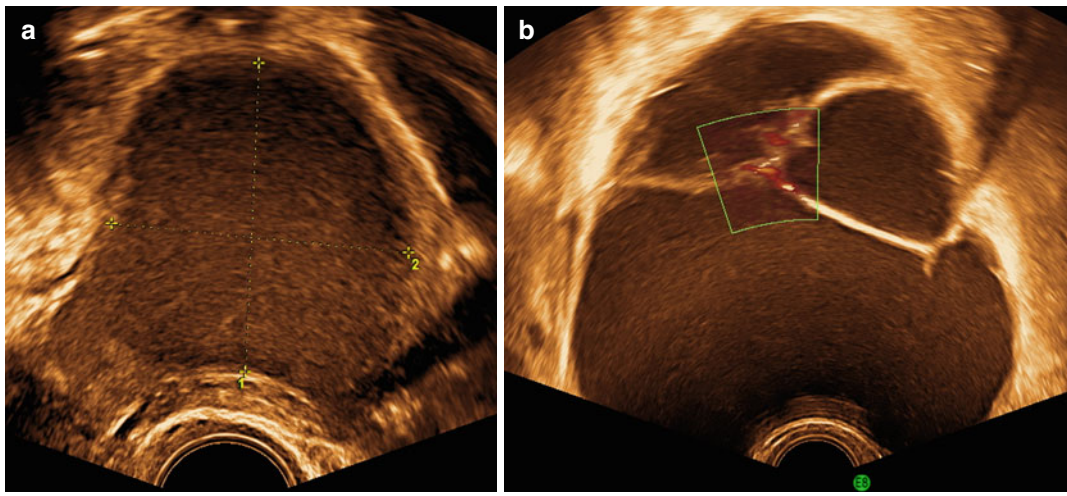

Fig. 1.6 A typical endometrioma (**a**) unilocular with ground glass appearance. (**b**) Benign mucinous cystadenoma, regular, multilocular cyst without solid components, with septae and minimal color score (2)

opposed to postmenopausal women. The simple rules (Table 1.5) will either classify the mass as benign, malignant, or not classifiable. Patients with adnexal masses classified as malignant should be treated by oncologists, while not classified tumors should be evaluated by specially trained sonographers (Ameye et al. 2012). For tumors, that are not classified the value of addition of 3D-TVS is questionable, although 3D-TVS was superior to conventional TVS for the prediction of malignant cases in a single study (Geomini et al. 2007). However, MRI may help in distinction between malignant and benign tumors (Dodge et al. 2012; Spencer and Ghattamaneni

2010; Spencer et al. 2010), which may be optimized further by DW MRI (Chou et al. 2012). For evaluation of tumor stage and recurrence CT, positron emission tomography – computed tomography (PET CT) may identify extra-ovarian disease (Dodge et al. 2012). Laparoscopy may be preferred (Whiteside and Keup 2009), when operative treatment is needed in adnexal masses classified as benign. Unclassified cysts have to be removed without spill, and oncologic expertise should be at hand.

1.4.4 Power Doppler at TVS for Evaluation of Uterus and Adnexal Mass

Power Doppler at TVS displays the overall vascularity and the pattern of the vessels.

The evaluation of color score is an additional parameter to the pattern palette at gray-scale evaluation in distinction between benign and malignant adnexal mass (Timmerman et al. 2010).

The power Doppler findings may vary in benign and malignant uterine mass (Hata et al. 1997; Szabo et al. 2002). In general, tumor vessels have an irregular chaotic pattern with numerous small and larger vessels and irregular branching, but several tumors have only scattered vessels (Szabo et al. 2002).

The circular flow around myomas is different from the perpendicular flow in adenomyosis (Chiang et al. 1999) in distinction between adenomyosis and myomas.

In the assessment of endometrial pathology, vessel pattern may have distinct features. The single vessel pattern indicate polyps and circular flow myomas, while an increased color score, and multiple vessel pattern (Alcazar et al. 2003; Epstein et al. 2002) are present in two-thirds of cases with endometrial malignancy. Examples are displayed in Fig. 1.7.

Calculation of vascularization index, flow index, and vascularization-flow index can be performed in a volume area of the 3D volume in the (VOCAL) post-processing system and may give an objective measurement of the color content, which is an observer-independent technique to evaluate increased tumor flow in the endometrium (Alcazar and Galvan 2009; Alcazar et al. 2006). However, quantification of vascularity at TVS is problematic, as this is dependent on standard settings of the software in different ultrasound machines (Alcazar 2008).

1.4.5 Dynamic Contrast-Enhanced MRI (DCE MRI) and Diffusion-Weighted MRI (DW MRI)

The features of DCE MRI are used in diagnosis and staging of malignant tumors (Kinkel et al. 2009; Bipat et al. 2003) and in indistinct pelvic mass (Kinkel et al. 2005). Unclassified ovarian and pelvic masses should primarily be seen by a trained sonographer, and when MRI is indicated, it should be performed by a MRI specialist in pelvic MRI. In distinction between degenerating leiomyomas and sarcomas early enhancement at MRI may suggest sarcomas (Goto et al. 2002; Shah et al. 2012; Wu et al. 2011). Moreover a combination of T2-weighted images and diffusion-weighted images is often helpful (Namimoto et al. 2009), as restricted diffusion is often seen in sarcomas. However, restricted diffusion may also be present in cellular leiomyomas, and No imaging technique has a high efficiency for a diagnosis of sarcomas. DW MRI may improve staging in endometrial and cervical cancer. It can also be helpful in characterizing complex adnexal masses and in depicting recurrent tumor after treatment of various gynecologic malignancies (Thoeny et al. 2012; Li et al. 2013; Chou et al. 2012).

1.4.5.1 DCE MRI in Therapeutic Imaging

DCE MRI is used to evaluate perfusion in myomas before and after UAE, RFA, and MRgFUS. Myomas with high extend of hyalinization and low vessel density had poor enhancement at DCE MRI (Shimada et al. 2004). The main object of all these newer methods is to achieve degenerative changes in myomas. Myomas without enhancement have often already had a spontaneous degeneration. Thus, myomas without significant perfusion may not benefit from UAE or MRgFUS (Nikolaidis et al. 2005; Al Hilli

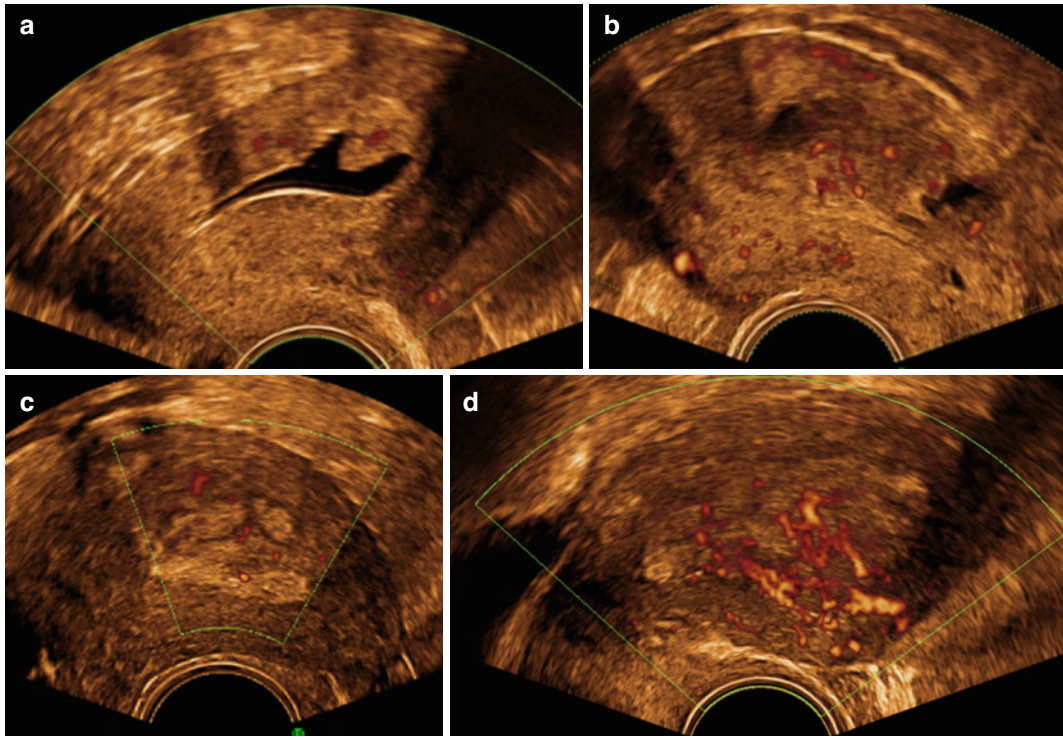

Fig. 1.7 Polyp (**a**), localized lesion with regular outline and one single small dominant vessel. (**b**) Adenomyosis, scattered, inhomogenic vessels in adenomyosis with large cystic areas in the myometrium and indistinct endomyometrial junction. (**c**) Endometrial cancer with heterogenic endometrium, irregular interrupted endomyometrial junction and scattered, not dominant large vessels. (**d**) An endometrial cancer with typical not scattered, not dominant multifocal vessels with abundant color score (4), and irregular branching

and Stewart 2010; Cura et al. 2006). Moreover, residual perfusion after treatment seems to be the most determined point for long-term effect of UAE or MRgFUS (Machtinger et al. 2012; Scheurig-Muenkler et al. 2012; Katsumori et al. 2008). At MRgFUS perfusion is normally evaluated immediately after treatment, and permanent efficient outcome is dependent on percentage of residual perfused myoma (Fig. 1.8). Contrast at MRI should never be used in patients with impaired renal function, where it may have serious complication (Marenzi et al. 2012) – and in these patients DW MRI can be used.

1.5 Evaluation of Congenital Uterine Abnormalities

In 3D TVS, the advantage of the coronal view makes it simple to diagnose the presence of either an arcuate, septate or bicorn uterus (Faivre et al. 2012). GIS may be added in indefinite findings. In the presence of more complex fusions anomalies especially in children, transabdominal ultrasound is the image modality, and MRI may add important information, as the resolution of MRI is higher than transabdominal ultrasound in the female pelvic.

1.6 Fertility Investigation

In the evaluation of subfertility TVS is the first step performed for evaluation of pathology in the uterus and ovary and for exclusion of a hydrosalpinx. Hydrosalpinx affects implantation in the endometrium (Strandell et al. 2001) and should be removed before fertility treatment (Camus et al. 1999). TVS is performed in the early follicular faze and may exclude most common uterine causes for subfertility (NICE.(04)). HY or SIS has higher diagnostic efficiency, and SIS may

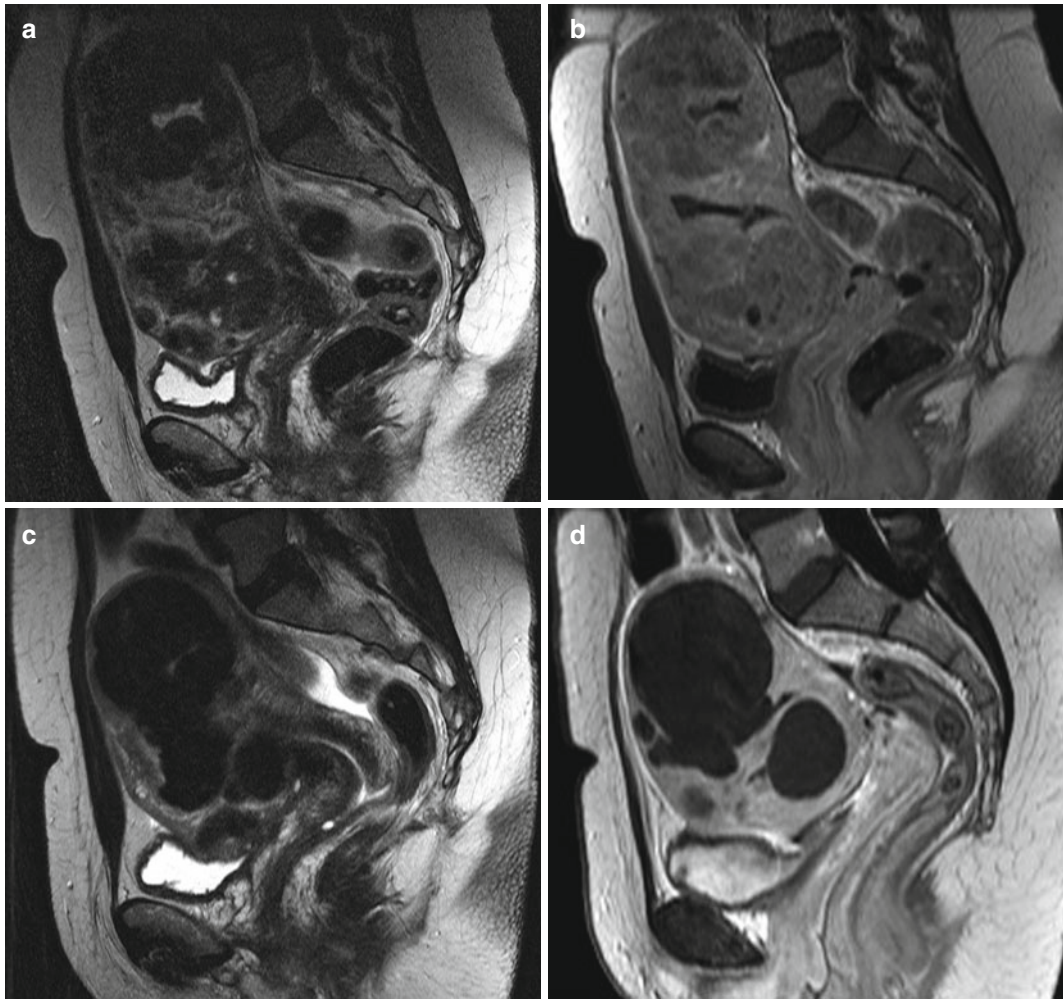

Fig. 1.8 T2-weighted MRI of myoma, (**a**) before UAE without contrast; (**b**) after contrast, where there is enhancement in myoma (*light colors*); (**c**) T2-weighted image 6 months after embolization with marked reduced volume of myoma; (**d**) 6 months after UAE after contrast, and there is no enhancement in myoma (*black*) – indicating complete embolization

be incorporated in the evaluation of tuba patency (see Sect. 1.6.1).

1.6.1 Tuba Factor

Traditionally tuba patency assessed by hysterosalpingography (HSG) has been replaced by hysterosalpingo-contrast sonography (HyCoSy). After a conventional scanning, a small uterine balloon catheter is placed in the uterine cavity, and the balloon inflated with saline is positioned just above the internal orificium. Saline is infused, and SIS is performed (Sect. 1.3.2). The intrauterine portion of the tube (proximal part) is localized. A contrast media containing air bubbles is introduced, and the passage of air bubbles through the proximal tube is observed at both sites. Free spill from the tube to the abdomen may be observed, but is not always optional. Passage of bubbles through the proximal tube, no hydrosalpinx observed and free fluid in the abdomen, after the examination has a high diagnostic efficiency for diagnosis of tuba patency (Chan et al. 2005; Holz et al. 1997).

The diagnostic efficiency of HyCoSy is dependent on training, and close to 50 scans is reported for sufficient efficiency (Dijkman et al. 2000). There might be slight but not substantial advantages of 3D-PDA (Sladkevicius et al. 2000; Kiyokawa et al. 2000). 3D-PDA may allow to capture a full volume of the tube and observe the spill, which seems to be the most optimal way to document the findings.

An alternative is transvaginal hydro laparoscopy, which will be dealt with in another chapter of the book.

1.7 Observer Variation

Endoscopy is a very observer-dependent technique, and the ability to recognizes and differentiate between normal and pathologic anatomy is part of the technical skill. This has raised attention on the difference in evaluation of anatomic structures even by trained surgeons (Buddingh et al. 2012). There is demonstrated considerable observer variation in the evaluation of adherences and endometriosis (Corson et al. 1995), and even for common benign diagnosis at HY (Kasius et al. 2011).

At TVS observer variation between different observers is substantial for diagnosis of adnexal mass (Sladkevicius and Valentin 2013), different abnormalities in the uterine cavity even in trained observers (Van den Bosch et al. 2012), and may be substantial when it comes to findings as adenomyosis (Dueholm et al. 2002c).

The observer variation at gynecologic MRI might also be substantial between MRI specialist with special training in pelvic pathology and other MRI specialists (Bazot et al. 2003).

Observer variation may be reduced by implementation of standard terms for definition, standards for image training, documentation and image conferences on findings. This is an important aspect to improve the diagnosis and treatment. There are large advances of TVS performed by surgeons in outpatient office settings, and with additional imaging added as outlined above. However, the widespread use may have an impact on image quality, and implementation of standardized terms should be elaborated in all imaging including endoscopy. Findings should be documented and conferences of imaging before and during endoscopy are quite obvious actions, which may increase the quality of surgery.

References

Abuhamad AZ, Singleton S, Zhao Y et al (2006) The Z technique: an easy approach to the display of the mid-coronal plane of the uterus in volume sonography. J Ultrasound Med 25:607–612

ACOG (2007) ACOG practice bulletin. Management of adnexal masses. Obstet Gynecol 110:201–214

Alcazar JL (2008) Three-dimensional power Doppler derived vascular indices: what are we measuring and how are we doing it? Ultrasound Obstet Gynecol 32:485–487

Alcazar JL, Galvan R (2009) Three-dimensional power Doppler ultrasound scanning for the prediction of endometrial cancer in women with postmenopausal bleeding and thickened endometrium. Am J Obstet Gynecol 200:44–46

Alcazar JL, Castillo G, Minguez JA et al (2003) Endometrial blood flow mapping using transvaginal power Doppler sonography in women with postmenopausal bleeding and thickened endometrium. Ultrasound Obstet Gynecol 21:583–588

Alcazar JL, Ajossa S, Floris S et al (2006) Reproducibility of endometrial vascular patterns in endometrial disease as assessed by transvaginal power Doppler sonography in women with postmenopausal bleeding. J Ultrasound Med 25:159–163

Al Hilli MM, Stewart EA (2010) Magnetic resonance-guided focused ultrasound surgery. Semin Reprod Med 28:242–249

Ameye L, Timmerman D, Valentin L et al (2012) Clinically oriented three-step strategy to the assessment of adnexal pathology. Ultrasound Obstet Gynecol 140:582–591

Angioni S, Loddo A, Milano F et al (2008) Detection of benign intracavitary lesions in postmenopausal women with abnormal uterine bleeding: a prospective comparative study on outpatient hysteroscopy and blind biopsy. J Minim Invasive Gynecol 15:87–91

Avila ML, Ruiz R, Cortaberria JR et al (2008) Assessment of cervical involvement in endometrial carcinoma by hysteroscopy and directed biopsy. Int J Gynecol Cancer 18:128–131

Bazot M, Cortez A, Darai E et al (2001) Ultrasonography compared with magnetic resonance imaging for the diagnosis of adenomyosis: correlation with histopathology. Hum Reprod 16:2427–2433

Bazot M, Darai E, de Clement GS et al (2003) Fast breath-hold T2-weighted MR imaging reduces interobserver variability in the diagnosis of adenomyosis. AJR Am J Roentgenol 180:1291–1296

Behera MA, Leong M, Johnson L et al (2010) Eligibility and accessibility of magnetic resonance-guided focused ultrasound (MRgFUS) for the treatment of uterine leiomyomas. Fertil Steril 94:1864–1868

Bettocchi S, Ceci O, Nappi L et al (2004) Operative office hysteroscopy without anesthesia: analysis of 4863 cases performed with mechanical instruments. J Am Assoc Gynecol Laparosc 11:59–61

Bipat S, Glas AS, van der Velden J et al (2003) Computed tomography and magnetic resonance imaging in staging of uterine cervical carcinoma: a systematic review. Gynecol Oncol 91:59–66

Buddingh KT, Morks AN, ten Cate Hoedemaker HO et al (2012) Documenting correct assessment of biliary anatomy during laparoscopic cholecystectomy. Surg Endosc 26:79–85

Caliskan E, Ozkan S, Cakiroglu Y et al (2010) Diagnostic accuracy of real-time 3D sonography in the diagnosis of congenital Mullerian anomalies in high-risk patients with respect to the phase of the menstrual cycle. J Clin Ultrasound 38:123–127

Camus E, Poncelet C, Goffinet F et al (1999) Pregnancy rates after in-vitro fertilization in cases of tubal infertility with and without hydrosalpinx: a meta-analysis of published comparative studies. Hum Reprod 14:1243–1249

Champaneria R, Abedin P, Daniels J et al (2010) Ultrasound scan and magnetic resonance imaging for the diagnosis of adenomyosis: systematic review comparing test accuracy. Acta Obstet Gynecol Scand 89:1374–1384

Chan CC, Ng EH, Tang OS et al (2005) Comparison of three-dimensional hysterosalpingo-contrast-sonography and diagnostic laparoscopy with chromopertubation in the assessment of tubal patency for the investigation of subfertility. Acta Obstet Gynecol Scand 84:909–913

Chiang CH, Chang MY, Hsu JJ et al (1999) Tumor vascular pattern and blood flow impedance in the differential diagnosis of leiomyoma and adenomyosis by color Doppler sonography. J Assist Reprod Genet 16:268–275

Chou CP, Chiou SH, Levenson RB et al (2012) Differentiation between pelvic abscesses and pelvic tumors with diffusion-weighted MR imaging: a preliminary study. Clin Imaging 36:532–538

Cicinelli E (2010) Hysteroscopy without anesthesia: review of recent literature. J Minim Invasive Gynecol 17:703–708

Cicinelli E, Parisi C, Galantino P et al (2003) Reliability, feasibility, and safety of minihysteroscopy with a vaginoscopic approach: experience with 6,000 cases. Fertil Steril 80:199–202

Cicinelli E, Marinaccio M, Barba B et al (2008) Reliability of diagnostic fluid hysteroscopy in the assessment of cervical invasion by endometrial carcinoma: a comparative study with transvaginal sonography and MRI. Gynecol Oncol 111:55–61

Corson SL, Batzer FR, Gocial B et al (1995) Intraobserver and inter-observer variability in scoring laparoscopic diagnosis of pelvic adhesions. Hum Reprod 10:161–164

Cura M, Cura A, Bugnone A (2006) Role of magnetic resonance imaging in patient selection for uterine artery embolization. Acta Radiol 47:1105–1114

de Kroon CD, de Bock GH, Dieben SW et al (2003) Saline contrast hysterosonography in abnormal uterine bleeding: a systematic review and meta-analysis. BJOG 110:938–947

de Kroon CD, Louwe LA, Trimbos JB et al (2004) The clinical value of 3-dimensional saline infusion sonography in addition to 2-dimensional saline infusion sonography in women with abnormal uterine bleeding: work in progress. J Ultrasound Med 23:1433–1440

Dijkman AB, Mol BW, van der Veen F et al (2000) Can hysterosalpingocontrast-sonography replace hysterosalpingography in the assessment of tubal subfertility? Eur J Radiol 35:44–48

Dodge JE, Covens AL, Lacchetti C et al (2012) Management of a suspicious adnexal mass: a clinical practice guideline. Curr Oncol 19:e244–e257

Dueholm M, Forman A, Jensen ML et al (2001a) Transvaginal sonography combined with saline contrast sonohysterography in evaluating the uterine cavity in premenopausal patients with abnormal uterine bleeding. Ultrasound Obstet Gynecol 18:54–61

Dueholm M, Lundorf E, Hansen ES et al (2001b) Evaluation of the uterine cavity with magnetic resonance imaging, transvaginal sonography, hysterosonographic examination, and diagnostic hysteroscopy. Fertil Steril 76:350–357

Dueholm M, Lundorf E, Hansen ES et al (2001c) Magnetic resonance imaging and transvaginal ultrasonography for the diagnosis of adenomyosis. Fertil Steril 76:588–594

Dueholm M, Lundorf E, Olesen F (2002a) Imaging techniques for evaluation of the uterine cavity and endometrium in premenopausal patients before minimally invasive surgery. Obstet Gynecol Surv 57:388–403

Dueholm M, Lundorf E, Hansen ES et al (2002b) Accuracy of magnetic resonance imaging and transvaginal ultrasonography in the diagnosis, mapping, and measurement of uterine myomas. Am J Obstet Gynecol 186:409–415

Dueholm M, Lundorf E, Sorensen JS et al (2002c) Reproducibility of evaluation of the uterus by transvaginal sonography, hysterosonographic examination, hysteroscopy and magnetic resonance imaging. Hum Reprod 17:195–200

Epstein E, Ramirez A, Skoog L et al (2001) Dilatation and curettage fails to detect most focal lesions in the uterine cavity in women with postmenopausal bleeding. Acta Obstet Gynecol Scand 80:1131–1136

Epstein E, Skoog L, Isberg PE et al (2002) An algorithm including results of gray-scale and power Doppler ultrasound examination to predict endometrial malignancy in women with postmenopausal bleeding. Ultrasound Obstet Gynecol 20:370–376

Faivre E, Fernandez H, Deffieux X et al (2012) Accuracy of three-dimensional ultrasonography in differ-

ential diagnosis of septate and bicornuate uterus compared with office hysteroscopy and pelvic magnetic resonance imaging. J Minim Invasive Gynecol 19:101–106

Garza Leal JG, Hernandez Leon I, Castillo SL et al (2011) Laparoscopic ultrasound-guided radiofrequency volumetric thermal ablation of symptomatic uterine leiomyomas: feasibility study using the halt 2000 ablation system. J Minim Invasive Gynecol 18:364–371

Geomini PM, Coppus SF, Kluivers KB et al (2007) Is three-dimensional ultrasonography of additional value in the assessment of adnexal masses? Gynecol Oncol 106:153–159

Goto A, Takeuchi S, Sugimura K et al (2002) Usefulness of Gd-DTPA contrast-enhanced dynamic MRI and serum determination of LDH and its isozymes in the differential diagnosis of leiomyosarcoma from degenerated leiomyoma of the uterus. Int J Gynecol Cancer 12:354–361

Hata K, Hata T, Maruyama R et al (1997) Uterine sarcoma: can it be differentiated from uterine leiomyoma with Doppler ultrasonography? A preliminary report. Ultrasound Obstet Gynecol 9:101–104

Holz K, Becker R, Schurmann R (1997) Ultrasound in the investigation of tubal patency. A meta-analysis of three comparative studies of Echovist-200 including 1007 women. Zentralbl Gynakol 119:366–373

Hudelist G, English J, Thomas AE et al (2011) Diagnostic accuracy of transvaginal ultrasound for non-invasive diagnosis of bowel endometriosis: systematic review and meta-analysis. Ultrasound Obstet Gynecol 37:257–263

Iversen H, Lenz S, Dueholm M (2012) Ultrasound-guided radiofrequency ablation of symptomatic uterine fibroids: short-term evaluation of effect of treatment on quality of life and symptom severity. Ultrasound Obstet Gynecol 40:445–451

Kaijser J, Bourne T, Valentin L et al (2013) Improving strategies for diagnosing ovarian cancer: a summary of the International Ovarian Tumor Analysis (IOTA) studies. Ultrasound Obstet Gynecol 41:9–20

Kasius JC, Broekmans FJ, Veersema S et al (2011) Observer agreement in the evaluation of the uterine cavity by hysteroscopy prior to in vitro fertilization. Hum Reprod 26:801–807

Katsumori T, Kasahara T, Kin Y et al (2008) Infarction of uterine fibroids after embolization: relationship between postprocedural enhanced MRI findings and long-term clinical outcomes. Cardiovasc Intervent Radiol 31:66–72

Kim CH, Kim SR, Lee HA et al (2011) Transvaginal ultrasound-guided radiofrequency myolysis for uterine myomas. Hum Reprod 26:559–563

Kinkel K, Kaji Y, Yu KK et al (1999) Radiologic staging in patients with endometrial cancer: a meta-analysis. Radiology 212:711–718

Kinkel K, Lu Y, Mehdizade A et al (2005) Indeterminate ovarian mass at US: incremental value of second imaging test for characterization–meta-analysis and Bayesian analysis. Radiology 236:85–94

Kinkel K, Forstner R, Danza FM et al (2009) Staging of endometrial cancer with MRI: guidelines of the European Society of Urogenital Imaging. Eur Radiol 19:1565–1574

Kiyokawa K, Masuda H, Fuyuki T et al (2000) Three-dimensional hysterosalpingo-contrast sonography (3D-HyCoSy) as an outpatient procedure to assess infertile women: a pilot study. Ultrasound Obstet Gynecol 16:648–654

Lasmar RB, Xinmei Z, Indman PD et al (2011) Feasibility of a new system of classification of submucous myomas: a multicenter study. Fertil Steril 95:2073–2077

Leone FP, Timmerman D, Bourne T et al (2010) Terms, definitions and measurements to describe the sonographic features of the endometrium and intrauterine lesions: a consensus opinion from the International Endometrial Tumor Analysis (IETA) group. Ultrasound Obstet Gynecol 35:103–112

Li W, Zhang Y, Cui Y et al (2013) Pelvic inflammatory disease: evaluation of diagnostic accuracy with conventional MR with added diffusion-weighted imaging. Abdom Imaging 38:193–200

Lotfallah H, Farag K, Hassan I et al (2005) One-stop hysteroscopy clinic for postmenopausal bleeding. J Reprod Med 50:101–107

Lykke R, Clevin L, Dueholm M (2012) A new technique for hysteroscopic resection of intramural myomas. J Gynecol Surg 28:147–149

Machtinger R, Inbar Y, Cohen-Eylon S et al (2012) MR-guided focus ultrasound (MRgFUS) for symptomatic uterine fibroids: predictors of treatment success. Hum Reprod 27:3425–3431

Makris N, Kalmantis K, Skartados N et al (2007) Three-dimensional hysterosonography versus hysteroscopy for the detection of intracavitary uterine abnormalities. Int J Gynaecol Obstet 97:6–9

Marenzi G, Cabiati A, Milazzo V et al (2012) Contrast-induced nephropathy. Intern Emerg Med 7(Suppl 3):181–183

Mavrelos D, Naftalin J, Hoo W et al (2011) Preoperative assessment of submucous fibroids by three-dimensional saline contrast sonohysterography. Ultrasound Obstet Gynecol 38:350–354

Meredith SM, Sanchez-Ramos L, Kaunitz AM (2009) Diagnostic accuracy of transvaginal sonography for the diagnosis of adenomyosis: systematic review and metaanalysis. Am J Obstet Gynecol 201:107.e1-6

Munro MG, Critchley HO, Fraser IS (2011) The FIGO classification of causes of abnormal uterine bleeding in the reproductive years. Fertil Steril 95:2204–2208

Nakai A, Koyama T, Fujimoto K et al (2008) Functional MR imaging of the uterus. Magn Reson Imaging Clin N Am 16:673–684, ix

Namimoto T, Yamashita Y, Awai K et al (2009) Combined use of T2-weighted and diffusion-weighted 3-T MR imaging for differentiating uterine sarcomas from benign leiomyomas. Eur Radiol 19:2756–2764

NICE. Fertility: assessment and treatment for people with fertility problems. National Institute for Clinical

Excellence (1-2-2004) [cited 1-11-2012]. Available from: http://www.rcog.org.uk
Nikolaidis P, Siddiqi AJ, Carr JC et al (2005) Incidence of nonviable leiomyomas on contrast material-enhanced pelvic MR imaging in patients referred for uterine artery embolization. J Vasc Interv Radiol 16:1465–1471
Paldino MJ, Barboriak DP (2009) Fundamentals of quantitative dynamic contrast-enhanced MR imaging. Magn Reson Imaging Clin N Am 17:277–289
Piscaglia F, Nolsoe C, Dietrich CF et al (2012) The EFSUMB guidelines and recommendations on the Clinical Practice of Contrast Enhanced Ultrasound (CEUS): update 2011 on non-hepatic applications. Ultraschall Med 33:33–59
Rabinovici J, David M, Fukunishi H et al (2010) Pregnancy outcome after magnetic resonance-guided focused ultrasound surgery (MRgFUS) for conservative treatment of uterine fibroids. Fertil Steril 93:199–209
Raine-Fenning NJ, Campbell BK, Clewes JS et al (2003) The reliability of virtual organ computer-aided analysis (VOCAL) for the semiquantification of ovarian, endometrial and subendometrial perfusion. Ultrasound Obstet Gynecol 22:633–639
Raine-Fenning NJ, Nordin NM, Ramnarine KV et al (2008) Evaluation of the effect of machine settings on quantitative three-dimensional power Doppler angiography: an in-vitro flow phantom experiment. Ultrasound Obstet Gynecol 32:551–559
RCOG. management of suspected ovarian masses in premenopausal women.GTG62. Royal College of Obstetricians and Gynaecologists (1-11-2011) [cited 25-10-2012]. Available from http://www.rcog.org.uk
Scheurig-Muenkler C, Koesters C, Grieser C et al (2012) Treatment failure after uterine artery embolization: prospective cohort study with multifactorial analysis of possible predictors of long-term outcome. Eur J Radiol 81:e727–e731
Shah SH, Jagannathan JP, Krajewski K et al (2012) Uterine sarcomas: then and now. AJR Am J Roentgenol 199:213–223
Shimada K, Ohashi I, Kasahara I et al (2004) Triple-phase dynamic MRI of intratumoral vessel density and hyalinization grade in uterine leiomyomas. AJR Am J Roentgenol 182:1043–1050
Sladkevicius P, Valentin L (2013) Intra- and inter-observer agreement when describing adnexal masses using the International Ovarian Tumour Analysis (IOTA) terms and definitions: a study on three-dimensional (3D) ultrasound volumes. Ultrasound Obstet Gynecol 41:318–327
Sladkevicius P, Ojha K, Campbell S et al (2000) Three-dimensional power Doppler imaging in the assessment of Fallopian tube patency. Ultrasound Obstet Gynecol 16:644–647
Sokalska A, Timmerman D, Testa AC et al (2009) Diagnostic accuracy of transvaginal ultrasound examination for assigning a specific diagnosis to adnexal masses. Ultrasound Obstet Gynecol 34:462–470
Spencer JA, Ghattamaneni S (2010) MR imaging of the sonographically indeterminate adnexal mass. Radiology 256:677–694
Spencer JA, Forstner R, Cunha TM et al (2010) ESUR guidelines for MR imaging of the sonographically indeterminate adnexal mass: an algorithmic approach. Eur Radiol 20:25–35
Spielmann AL, Keogh C, Forster BB et al (2006) Comparison of MRI and sonography in the preliminary evaluation for fibroid embolization. AJR Am J Roentgenol 187:1499–1504
Spies JB, Spector A, Roth AR et al (2002) Complications after uterine artery embolization for leiomyomas. Obstet Gynecol 100:873–880
Stewart EA, Gostout B, Rabinovici J et al (2007) Sustained relief of leiomyoma symptoms by using focused ultrasound surgery. Obstet Gynecol 110:279–287
Strandell A, Lindhard A, Waldenstrom U et al (2001) Hydrosalpinx and IVF outcome: cumulative results after salpingectomy in a randomized controlled trial. Hum Reprod 16:2403–2410
Szabo I, Szantho A, Csabay L et al (2002) Color Doppler ultrasonography in the differentiation of uterine sarcomas from uterine leiomyomas. Eur J Gynaecol Oncol 23:29–34
Taran FA, Hesley GK, Gorny KR et al (2010) What factors currently limit magnetic resonance-guided focused ultrasound of leiomyomas? A survey conducted at the first international symposium devoted to clinical magnetic resonance-guided focused ultrasound. Fertil Steril 94:331–334
Thoeny HC, Forstner R, De KF (2012) Genitourinary applications of diffusion-weighted MR imaging in the pelvis. Radiology 263:326–342
Timmerman D, Valentin L, Bourne TH et al (2000) Terms, definitions and measurements to describe the sonographic features of adnexal tumors: a consensus opinion from the International Ovarian Tumor Analysis (IOTA) Group. Ultrasound Obstet Gynecol 16:500–505
Timmerman D, Ameye L, Fischerova D et al (2010) Simple ultrasound rules to distinguish between benign and malignant adnexal masses before surgery: prospective validation by IOTA group. BMJ 341:c6839
Timmermans A, Opmeer BC, Khan KS et al (2010) Endometrial thickness measurement for detecting endometrial cancer in women with postmenopausal bleeding: a systematic review and meta-analysis. Obstet Gynecol 116:160–167
Van CB, Timmerman D, Valentin L et al (2012a) Triaging women with ovarian masses for surgery: observational diagnostic study to compare RCOG guidelines with an International Ovarian Tumour Analysis (IOTA) group protocol. BJOG 119:662–671
Van HC, Van CB, Bourne T et al (2012b) External validation of diagnostic models to estimate the risk of malignancy in adnexal masses. Clin Cancer Res 18:815–825

Van den Bosch T, Valentin L, Van SD et al (2012) Detection of intracavitary uterine pathology using offline analysis of three-dimensional ultrasound volumes: interobserver agreement and diagnostic accuracy. Ultrasound Obstet Gynecol 40:459–463

van Hanegem N, Breijer MC, Khan KS et al (2011) Diagnostic evaluation of the endometrium in postmenopausal bleeding: an evidence-based approach. Maturitas 68:155–164

Walker WJ, Barton-Smith P (2006) Long-term follow up of uterine artery embolisation–an effective alternative in the treatment of fibroids. BJOG 113:464–468

Walker WJ, Carpenter TT, Kent AS (2004) Persistent vaginal discharge after uterine artery embolization for fibroid tumors: cause of the condition, magnetic resonance imaging appearance, and surgical treatment. Am J Obstet Gynecol 190:1230–1233

Whiteside JL, Keup HL (2009) Laparoscopic management of the ovarian mass: a practical approach. Clin Obstet Gynecol 52:327–334

Wu TI, Yen TC, Lai CH (2011) Clinical presentation and diagnosis of uterine sarcoma, including imaging. Best Pract Res Clin Obstet Gynaecol 25:681–689

Yaman C, Sommergruber M, Ebner T et al (1999) Reproducibility of transvaginal three-dimensional endometrial volume measurements during ovarian stimulation. Hum Reprod 14:2604–2608

Zhou XD, Ren XL, Zhang J et al (2007) Therapeutic response assessment of high intensity focused ultrasound therapy for uterine fibroid: utility of contrast-enhanced ultrasonography. Eur J Radiol 62:289–294